LANGMUIR

pubs.acs.org/Langmuir Article

Antifouling Polymer Brushes via Oxygen-Tolerant Surface-Initiated PET-RAFT

Andriy R. Kuzmyn, Ai T. Nguyen, Lucas W. Teunissen, Han Zuilhof,* and Jacob Baggerman*

Cite This: *Langmuir* 2020, 36, 4439−4446 Read Online

ACCESS | Metrics & More | Article Recommendations | Supporting Information

ABSTRACT: This work presents a new method for the synthesis of antifouling polymer brushes using surface-initiated photoinduced electron transfer-reversible addition−fragmentation chain-transfer polymerization with eosin Y and triethanolamine as catalysts. This method proceeds in an aqueous environment under atmospheric conditions without any prior degassing and without the use of heavy metal catalysts. The versatility of the method is shown by using three chemically different monomers: oligo(ethylene glycol) methacrylate, *N*-(2-hydroxypropyl)methacrylamide, and carboxybetaine methacrylamide. In addition, the light-triggered nature of the polymerization allows the creation of complex three-dimensional structures. The composition and topological structuring of the brushes are confirmed by X-ray photoelectron spectroscopy and atomic force microscopy. The kinetics of the polymerizations are followed by measuring the layer thickness with ellipsometry. The polymer brushes demonstrate excellent antifouling properties when exposed to single-protein solutions and complex biological matrices such as diluted bovine serum. This method thus presents a new simple approach for the manufacturing of antifouling coatings for biomedical and biotechnological applications.

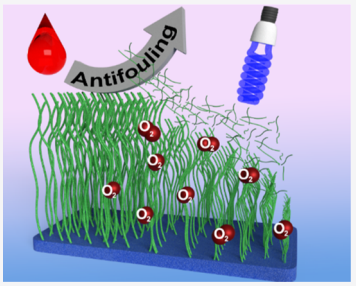

INTRODUCTION

Nonspecific interactions between engineering materials and complex biological fluids obstruct the performance of many biotechnological and biomedical devices.[1,2] In particular, nonspecific adsorption of protein or fouling from biological media can cause issues such as blockage of flow-through separation columns and porous membranes,[3] nonspecific response of label-free affinity-based biosensors,[1,4] reduced circulation time of nanocarriers in the bloodstream,[5] and bacterial attachment on contact lenses.[6,7] The fouling can be curbed by introducing antifouling coatings on the surfaces of the materials that are in contact with a biological matrix.[1,2,8−10] The creation of these coatings that can resist nonspecific interactions with a biological medium still poses a challenge, in particular their formation in mass manufacturing processes.[1,8,11,12]

Numerous approaches to create antifouling coatings have been developed, for example, based on self-assembled monolayers[13] and "grafted to"[14,15] and "grafted from"[1,2,8,9,11,12,16−22] polymer coatings. Although self-assembled monolayers and "grafted to"-polymer layers can decrease adsorption from single-protein solutions, most of them fail when contacted with complex biological matrices, such as blood serum or cells.[13−15] The introduction of surface-initiated living radical polymerization (SI-LRP) provided a new efficient instrument to form antifouling layers based on "grafted from"-polymer brushes.[23] For instance, polymer brushes based on oligo(ethylene glycol) methacrylate,[2,9,18] *N*-(2-hydroxypropyl) methacrylamide (HPMA),[20,22,24] carboxybetaine methacrylamide (CBMA),[2,9,17,20,24,25] sulfobetaine methacrylamide,[10,21,26] and their derivatives have shown remarkable resistance to nonspecific adsorption of proteins and also cells from complex biological fluids. Surface-initiated atom-transfer radical polymerization (SI-ATRP) is the most commonly applied SI-LRP method thus far.[1,2,8,19,20,27] The well-controlled nature of SI-ATRP allows to tune the thickness and density of polymer brushes in order to achieve the best resistance to nonspecific protein adsorption.[23,28] The versatility of SI-ATRP allowed to grow polymer brushes from almost any type of surfaces.[29] However, the SI-ATRP technique uses relatively high concentrations of metal-based catalysts to generate radicals from alkyl halides,[8,10,18,20,21] provides limited means to structure the brush layer in either composition or thickness, and requires a rigorous control over an oxygen-free atmosphere to perform the reaction. Therefore, new approaches have been developed to overcome these limitations.

An approach based on single-electron transfer living radical polymerization (SET-LRP) strongly reduced the amount of Cu^0 needed to conduct the polymerization.[22] Recently, our group introduced the use of light-triggered living radical polymerization (LT-LRP) using an iridium-based catalyst,

Received: November 14, 2019
Revised: April 3, 2020
Published: April 15, 2020

https://dx.doi.org/10.1021/acs.langmuir.9b03536
Langmuir 2020, 36, 4439−4446

which allowed to control the thickness and functionality of antifouling polymer brushes in a spatial manner (via patterning) and over time (via intensity and duration of the illumination). This thus opened up the possibility to create micropatterned antifouling bioactive layers with a controlled thickness and functionality per pattern.[24] However, the third limitation still remains: despite the well-controlled and tunable nature of SI-ATRP, SET-LRP, and LT-LRP, they all require an oxygen-free environment during the polymerization.[8,9,11,12,18,20,22,24] This also applies to novel surface-initiated approaches based on reversible addition−fragmentation chain transfer (RAFT)[30] and photoiniferter-mediated polymerization (PIMP):[31−33] no heavy metal catalysts are required, and a wide compatibility with a large number of monomers exists, but they still require oxygen-free conditions to sustain the controlled radical polymerization.

Recently, a new RAFT-based technique was introduced: photoinduced electron transfer-RAFT (PET-RAFT).[34−37] This method allowed to synthesize polymers in a controlled fashion in the presence of oxygen. The mechanism and living nature of PET-RAFT polymerizations were previously investigated by Xu et al.[38] They proposed that the reaction proceeds according to a reductive quenching cycle of eosin Y (EY) in which triethanolamine (TEOA) acts as a sacrificing electron donor to reduce oxygen in the polymerization system. The reduction of oxygen allows the polymerization to proceed in an oxygen-containing environment. In addition, the mild conditions and water compatibility enabled the synthesis of polymer grafting of polymer chains from a DNA and living cells.[35,36] Moreover, it was recently shown that this method is also suitable for surface-initiated polymerization of polymer brushes.[37]

Herein, we show the synthesis of antifouling polymer brushes employing surface-initiated PET-RAFT (SI-PET-RAFT). We demonstrate that this method is suitable for growing brushes in water with an accessible and affordable organic photocatalyst, EY. The applied technique is thus free from heavy metals. We have synthesized polymer brushes based on three different types of antifouling monomers: oligo(ethylene glycol) methacrylate (MeOEGMA), HPMA, and CBMA (see Scheme 1), as these represent three main chemical approaches toward minimizing the nonspecific adsorption of proteins by polymer brushes. Moreover, we aimed for a truly robust method that should allow polymerization in two- and three-dimensional patterns of all three of those chemically different monomers in oxygen-tolerant conditions. The composition, thickness, and pattern formation of the resulting brushes were characterized extensively by X-ray photoelectron spectroscopy (XPS), atomic force microscopy (AFM), and imaging ellipsometry. The antibiofouling properties of the synthesized polymer brushes were analyzed using fluorescence confocal laser scanning microscopy (CLSM) of surfaces exposed to single-fluorescent protein solutions and bovine serum (BS).

EXPERIMENTAL SECTION

Materials. All chemical reagents were used without further purification, unless otherwise specified. 4-Cyano-4-(phenylcarbonothioylthio)pentanoic acid *N*-succinimidyl ester (RAFT-NHS), (3-aminopropyl)triethoxysilane (APTES), TEOA, EY, triethylamine (TEA), oligo(ethylene glycol) methyl ether methacrylate (MeOEGMA, average M_n 300), ethanol (EtOH, 99.9%), acetone (99.5%), dry tetrahydrofuran (THF, 99.9%), and phosphate-buffered saline (PBS) were purchased from Sigma-Aldrich; HPMA was obtained from Polysciences, Inc.; and streptavidin-Alexa488 conjugate (Str-Alexa488) and BS albumin-Alexa488 conjugate (BSA-Alexa488) were purchased from Fisher Thermo Scientific. Silicon substrates were acquired from Siltronix. Deionized water was produced using a Milli-Q integral 3 system (Millipore, Molscheim, France). (3-Acryloylamino-propyl)-(2-carboxy-ethyl)-dimethyl-ammonium (CBMA) was synthesized according to a previously described procedure.[11,12,20] BS was obtained and biotinylated as previously described.[21]

Scheme 1. Schematic Depiction of the Air-Tolerant SI-PET-RAFT Technique To Make Antifouling Polymer Brushes

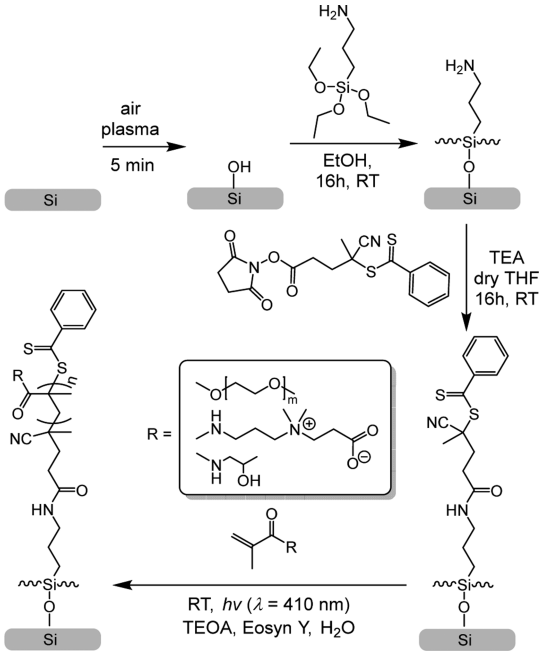

Light Source. Light-emitting diodes (LEDs) with a maximum intensity at 410 nm (Intelligent LED Solutions product number: ILH-XO01-S410-SC211-WIR200) were used, and the current was set at 700 mA, corresponding to a total radiometric power of 2.9 W, according to the manufacturer's specifications.

Formation of RAFT Agent-Functionalized Monolayers. The substrates were rinsed with acetone, absolute ethanol (EtOH), and Milli-Q water and blown dry under a gentle stream of Ar. Subsequently, the surfaces were exposed to an oxygen plasma for 5 min in a plasma cleaner (100 W; 5 mbar O_2; Diener electronic GmbH, Germany). The freshly activated surfaces were immediately immersed in a freshly prepared solution of APTES (1 mg·mL^{-1}) in EtOH at room temperature (RT) for 16 h. The substrates were subsequently rinsed with EtOH and Milli-Q water and blow-dried with Ar. After immobilization of APTES on surfaces, the substrates were submerged in a solution of RAFT-NHS (20 mg, 53 μmol) and TEA (7 mg, 10 μL, 72 μmol) in 1 mL of dry THF at RT for 16 h. The substrates were subsequently rinsed with THF, acetone, EtOH, and Milli-Q water and blow-dried with Ar. The substrates were stored under Ar protection before use.

SI-PET-RAFT Synthesis of Polymer Brushes. A stock solution consisting of a photocatalyst was prepared containing EY (25 mg, 39 μmol) and TEOA (160 mg, 1.6 mmol) in 10 ml of Milli-Q water. The monomer HPMA (178 mg, 1.3 mmol) or MeOEGMA (94 mg, 0.3 mmol) or CBMA (76 mg, 0.3 mmol) was dissolved in Milli-Q water (1 mL), and subsequently, 10 μL of the stock solution was added. The mixture was vortexed and added to the vials containing surfaces with the immobilized RAFT agent. Immediately after this, the polymerization was conducted by irradiating the vials with visible light from a LED light source for different periods of time. The height of polymerization solution on top of the surfaces was 2 mm. In these experiments, the light source was placed 3−4 cm from the substrates (Figure S1) to prevent substantial heating of the samples with the

https://dx.doi.org/10.1021/acs.langmuir.9b03536
Langmuir 2020, 36, 4439−4446

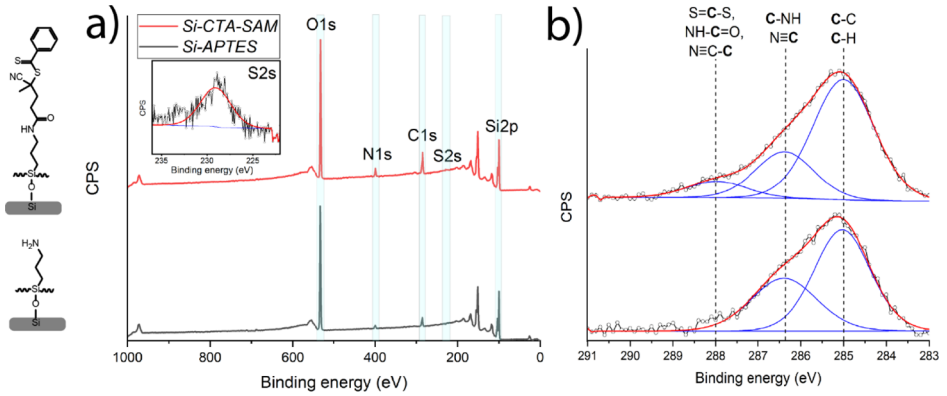

Figure 1. XPS characterization of the APTES- and initiator-functionalized monolayers. (a) Wide-scan spectra of the APTES- (gray line) and initiator-functionalized monolayers (red line); the inset shows the narrow-scan spectrum of the S 2s region. (b) Corresponding narrow-scan C 1s spectra.

light. The polymerization was stopped by turning off the light. The samples were removed from the solution and subsequently rinsed with Milli-Q water and ethanol and blown dry under a stream of Ar.

X-ray Photoelectron Spectroscopy. XPS measurements were performed using a JPS-9200 photoelectron spectrometer (JEOL Ltd., Japan). All the samples were prepared and stored under ambient conditions prior to analysis using a focused monochromated Al Kα X-ray source (spot size of 300 μm) radiation at 12 kV and 20 mA with an analyzer energy pass of 10 eV. XPS wide-scan and narrow-scan spectra were obtained under UHV conditions (base pressure 3×10^{-7} Torr). All narrow-range spectra were corrected with a linear background before fitting. The spectra were fitted with symmetrical Gaussian/Lorentzian [GL(30)] line shapes using CasaXPS. All spectra were referenced to the C 1s peak attributed to C−C and C−H atoms at 285.0 eV.

Static Water Contact Angle Measurements. The wettability of the modified surfaces was determined by automated static water contact angle measurements with the use of a Kruss DSA 100 goniometer. The volume of a drop of demineralized water is 3 μL. Contact angles from sessile drops measured by the tangent method were estimated using a standard error propagation technique involving partial derivatives.

Spectroscopic Ellipsometry. The polymerization kinetics were followed by measuring the dry thickness of the brushes using an Accurion Nanofilm_ep4 imaging ellipsometer. The ellipsometric data were acquired in air at RT using light in the wavelength range of λ = 400.6−761.3 nm at an angle of incidence of 50°. The data were fitted with EP4 software using a multilayer model.

Atomic Force Microscopy. AFM surface topography images were acquired by an Asylum Research MFP-3D SA AFM (Oxford Instruments, United Kingdom). Gwyddion software was used to process and analyze the AFM topography images.[39]

Fluorescence Microscopy. A Leica TCS SP8 confocal laser scanning microscope (Leica Microsystems, Mannheim, Germany) was used to measure protein fouling and specific interactions of the coated surfaces. A Leica HyDTM hybrid detector was used in photon counting mode to measure the intensity of the fluorescence signal. A 10× objective was used, and the samples were set in focus by maximizing the reflected light intensity from the laser. Fluorescence images were obtained by accumulating 10 consecutive images. Images were analyzed with the Leica LAS X Life Science software.

Protein Fouling Studies. Fouling of the coated surfaces by individual proteins or in complex biological media was investigated by incubating surfaces in a single-protein solution of Str-Alexa488 (0.5 mg·mL^{-1}) or BSA-Alexa488 (0.5 mg·mL^{-1}) or in a 10% dilution biotinylated BS for 15 min at RT. The surfaces were then washed with PBS (10 mL, pH 7.4). The samples exposed to biotinylated BS were further labeled, followed by exposure to Str-Alexa (0.5 mg·mL^{-1}) for 15 min at RT. Afterward, the samples were again rinsed with PBS (10 mL, pH 7.4) and Milli-Q water (10 mL) and subsequently dried by blowing with Ar. Further, the samples were mounted on the glass slides, and the fluorescence intensity of adsorbed proteins was measured.

The limit of detection was determined by placing 1 μL droplets containing known concentrations of BSA-Alexa488 on plasma-cleaned silicon oxide surfaces. The droplets were allowed to dry. The spot sizes of the dried drops were measured, allowing to calculate the surface density of the dried protein in ng·mm^{-2}. The fluorescence intensity of the spots was measured according to the method described above.

Electronic Core-Level Calculations. All calculations were done with the Gaussian 16 program.[40] The geometries of the different systems were optimized at the B3LYP/6-311G(d,p) level of theory. Natural bond orbital (NBO) analysis was employed to obtain the core orbital energies.[41]

RESULTS AND DISCUSSION

Synthesis of Initiator-Coated Surfaces. The antifouling polymer brushes were created in four steps starting from bare silicon surfaces (Scheme 1). The surfaces were first coated with a RAFT agent-functionalized monolayer, which was then used for surface-initiated polymerization of the brushes. To this aim, bare silicon surfaces were first oxidized using an air plasma for 5 min and subsequently coated with APTES. The amine-terminated surfaces were reacted with RAFT-NHS, yielding a RAFT agent-functionalized monolayer. From the RAFT agent-coated surfaces, antifouling polymer brushes were grown using SI-PET-RAFT in the presence of EY and TEOA as catalysts based on MeOEGMA (average M_n 300), HPMA, and CBMA. We will now discuss each step in detail.

The silicon surfaces were functionalized with the initiator in two stages. First, the silicon surfaces were functionalized with APTES. The successful modification with APTES was confirmed with XPS. The XPS wide-scan spectrum showed main peaks that correspond to O 1s, C 1s, N 1s, and Si 2p atoms (Figure 1a). The experimental ratio between C and N was 4.3:1.0, which is slightly higher than the theoretical elemental ratio in the compound (3:1), which is attributed to atmospheric contamination. The high content of oxygen in the XPS spectrum confirms the presence of a thin silicon oxide layer. The XPS narrow-scan spectrum of the C 1s region (Figure 1b) can be deconvoluted with two peaks. The peak at 285.0 eV is attributed to the carbon atoms in the alkyl backbone of APTES, and the peak at 286.5 eV is assigned to the carbon atoms adjacent to the amino group [C−N]. The observed ratio between the [C−C/H] and [C−N] peaks is

https://dx.doi.org/10.1021/acs.langmuir.9b03536
Langmuir 2020, 36, 4439−4446

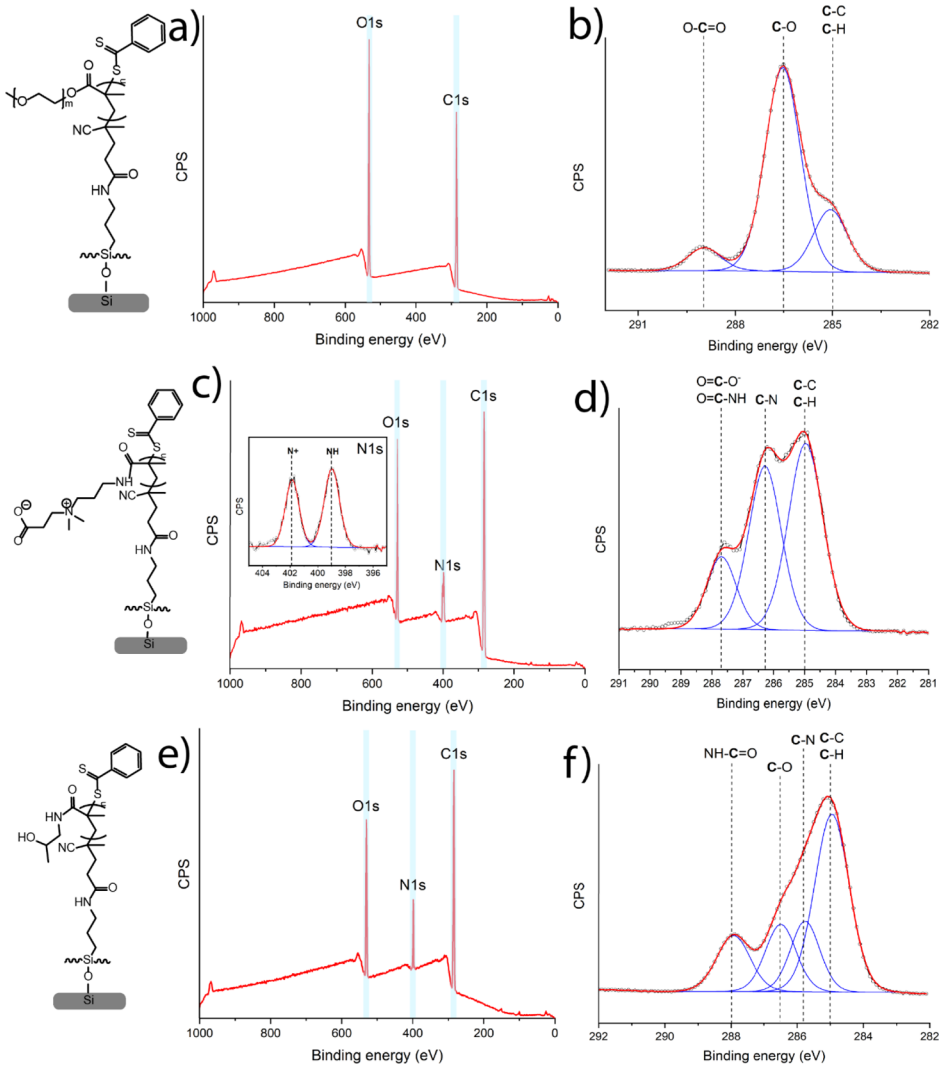

Figure 2. XPS characterization of poly(MeOEGMA) brushes: (a) wide-scan spectrum and (b) narrow-scan C 1s spectrum. Poly(CBMA) brushes: (c) wide-scan spectrum with the narrow-scan spectrum (inset) of the N 1s region and (d) narrow-scan C 1s spectrum. Poly(HPMA) brushes: (e) wide-scan spectrum and (f) narrow-scan C 1s spectrum.

1.7:1.0, which is comparable to the theoretical ratio of 2:1 between [**C**−C/H] and [**C**−N]. The XPS spectrum of the C 1s region of the APTES monolayer is also in agreement with the predicted XPS spectrum based on calculated core orbital energy levels, as obtained by density functional theory (DFT) calculations (Figure S2).[42,43] The XPS wide-scan spectrum also allowed to estimate the thickness of the APTES monolayer based on the Si/C ratio.[44] This thickness was estimated to be 0.5 ± 0.1 nm, in line with expectations for an APTES monolayer.

The initiator-functionalized surfaces were created by exposing previously prepared APTES-modified surfaces to RAFT-NHS (Scheme 1). The reaction was conducted in dry THF in the presence of TEA. The success of the reaction was confirmed by XPS. In the XPS wide-scan spectrum, the main peaks can be observed, which correspond to O 1s, C 1s, N 1s, S 2s, and Si 2p atoms with a ratio of 5.2:1.0:0.4 for C/N/S. The theoretical ratio for these elements is 8.0:1.0:1.0 in the case of a 100% conversion of the reaction between APTES and RAFT-NHS. Based on the C/N ratio obtained from eight samples, 29 ± 4% of the surface-bound amines has reacted to hold an RAFT agent moiety (eq S1). This was confirmed by the narrow-range C 1s spectrum, which can be fitted with three major peaks attributed to [**C**−C/H] at 285.0 eV, [**C**−NH, N≡**C**] at 286.4 eV, and [S=**C**−S, NH−**C**=O, N≡**C**−**C**] at 288.X eV. DFT-based simulations of the C 1s spectrum agree with this peak assignment (Figure S3).[42,43] In addition, the presence of sulfur was clearly shown in the XPS S 2s narrow-scan spectrum (Figure 1a, inset) with a peak maximum at 228 eV, indicating the presence of the RAFT agent on the surface. These results are in accordance with the previously published XPS spectra of the RAFT agent.[30] The thickness of the obtained layer has increased in comparison with that of the APTES monolayer and was calculated to be 1.1 ± 0.2 nm based on the C/Si ratio. Moreover, the static water contact angle of the coated surfaces before and after RAFT-NHS modification increased from 54 ± 1 to 97 ± 1°. Altogether, these characterizations confirm the successful immobilization of the RAFT agent on the silicon oxide surfaces.

Synthesis and Characterization of Poly(MeOEGMA), Poly(CBMA), and Poly(HPMA) Brushes. Poly(HPMA), poly(MeOEGMA), and poly(CBMA) brushes with different thicknesses were grown from the RAFT agent-coated surfaces by SI-PET-RAFT using EY as a photocatalyst. EY was used

https://dx.doi.org/10.1021/acs.langmuir.9b03536
Langmuir 2020, 36, 4439−4446

because it has been shown to be an oxygen-tolerant photocatalyst for polymerizations.[45] The polymerizations were conducted in Milli-Q water solution in the presence of TEOA. The AFM topography images of brush-coated surfaces through the range of the thicknesses from 4 to 45 nm revealed highly homogeneous layers with roughnesses of R_q = 0.36 ± 0.03 nm for poly(HPMA), R_q = 0.14 ± 0.04 nm for poly(MeOEGMA), and R_q = 0.50 ± 0.18 nm for poly(CBMA). The chemical composition of each synthesized polymer brush was confirmed by XPS (only layers >20 nm thickness are discussed so as to minimize the effects of the underlying Si surface and original APTES monolayer). The XPS wide-scan spectrum of a poly(MeOEGMA) layer with a thickness of 27 nm, as determined by ellipsometry, showed two main peaks for O 1s and C 1s in a ratio of 1.0:2.6 (Figure 2a). The XPS narrow-scan spectrum of the C 1s region shows three main peaks of carbon atoms: [**C**−C/H]/[**C**−O]/[O−**C**═O] in a ratio of 2.8:9.4:1 (Figure 2b). In addition, this C 1s narrow spectrum was simulated for two MeOEGMA monomers (Figure S3), with an average M_w of 300 (M_w = 278.35 and M_w = 322.40). The simulated spectrum gives a ratio between [**C**−C/H], [**C**−O], and [O−**C**═O] of 3:10:1, which is in good agreement with the ratio found by fitting the experimental data.[42,43] The static water contact angle of poly(MeOEGMA)-coated surfaces was determined to be 49 ± 1°, indicating the formation of a hydrophilic layer. In summary, the XPS, AFM, and contact angle data confirm the presence of well-defined poly(MeOEGMA) brushes.

The XPS wide-scan spectrum of poly(CBMA) brushes with an ellipsometric thickness of 29 nm (Figure 3c) shows three main peaks related to O, N 1, and C atoms in a ratio of 2.6:1.8:12.6. This indicates an enhanced carbon content compared to the expected ratio based on the elemental composition of the poly(CBMA) structure: 3:2:12 because of atmospheric contamination. The zwitterionic nature of poly(CBMA) brushes was also confirmed by the XPS narrow-scan spectrum of the N 1s region that displays two chemically different types of nitrogen atoms [N^+] and [NH] in a ratio of 1:1.3. The deviation from 1:1 ratio seems to be an XPS-induced change, as noted by van Andel et al.[21] The narrow-scan XPS C 1s spectrum (Figure 2d) displays two broad peaks at 285.0 and 286.3 eV assigned to [**C**−C/H] and [**C**−N] atoms and a smaller peak at 287.7 eV attributed to the carbonyl and carboxyl atoms. The ratio between the [**C**−C/H], [**C**−N], and [**C**═O] peaks is 5.5:4.6:1.8, which indicates a relatively high aliphatic carbon content compared to the theoretically expected composition of the poly(CBMA) structure (5:5:2). The poly(CBMA) layers also showed high hydrophilicity with a static water contact angle of 20 ± 1°. The overall physicochemical characterization for the poly(CBMA) layers is in good agreement with the properties found for poly(CBMA) layers synthesized using other polymerization methods such as ATRP and PIMP.[2,11,12,20,21,33]

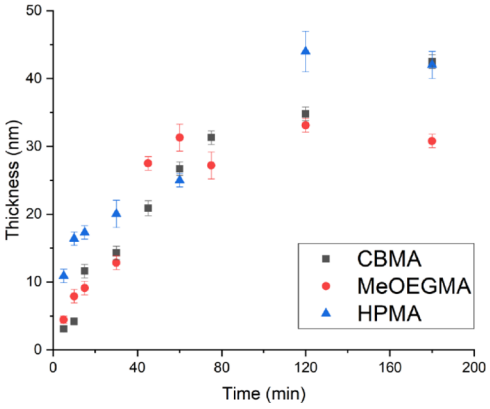

Figure 3. Dry thickness of poly(MeOEGMA), poly(CBMA), and poly(HPMA) brushes as a function of the polymerization time, as determined by ellipsometry.

The chemical composition of poly(HPMA) brushes was also confirmed by XPS. The XPS wide-scan spectrum of poly(HPMA) brushes with an ellipsometric thickness of 26 nm (Figure 2e) shows three main peaks related to O 1s, N 1s, and C 1s electrons in a 1.8:1:7.6 ratio, which is in agreement with the elemental composition of the poly(HPMA) structure (2:1:7). The narrow-scan XPS C 1s spectrum (Figure 2c) displays a broad peak at 285.X eV, with a shoulder between 286 and 287 eV, attributed to overlapping signals from aliphatic, alcohol, and amine carbon atoms, and a smaller peak at 288.2 eV attributed to the carbonyl atom. The spectrum was deconvoluted by fitting it with four peaks at 285.0 eV assigned to aliphatic [C−H] and [C−C] atoms, at 285.7 eV from the [C−N] atoms, at 286.6 eV from the [C−O] atoms, and at 288.2 eV from the NH−C═O atoms. The fitted ratio between the [C−C/H], [C−N], [C−O], and [C═O] peaks is 3.6:1.2:1.2:1.1, which correlates with the theoretically expected composition of the poly(HPMA) structure (4:1:1:1). Accurate fitting is in this case difficult because of the overlap between the [C−C/H], [C−N], and [C−O] peaks, in line with the previously reported experimental and simulated C 1s XPS spectra.[24] The poly(HPMA) brushes displayed a static water contact angle of 49 ± 1°, confirming the formation of a hydrophilic brush. In summary, well-defined poly(HPMA) brushes could also be made by this SI-PET-RAFT method, yielding characteristics that correspond to that of analogous coatings made by other methods, such as SET-LRP,[22] ATRP,[20] and LT-LRP.[24]

Kinetics of Polymer Brush Growth. The kinetics of the polymer brush growth for all three monomers were followed by measuring the polymer brush layer thicknesses with scanning ellipsometry (Figure 3). The polymer brushes all demonstrated a linear growth in the first hour, which indicates the controlled nature of the polymerization. This allows tuning of the polymer brush thickness from 0 to 40 nm and reaching thicknesses higher than 10 nm within the first 20 min of polymerization under ambient conditions, that is, in an oxygen-containing environment. Thicknesses higher than 10−15 nm are required for significant resistance toward nonspecific adsorption from complex biological matrices by polymer brushes based on antifouling monomers such MeOEGMA, HPMA, and CBMA.[18,20,21] The rate of polymerization during the first hour for poly(MeOEGMA), poly(HPMA), and poly(CBMA) was determined to be 0.44 ± 0.04, 0.51 ± 0.05, and 0.21 ± 0.04 nm·min^{-1}, respectively. [Note: The concentration of the HPMA monomer was increased 4 times in comparison with that of CBMA and MeOEGMA. Lower monomer concentrations of HPMA did not allow to create brushes thicker than 14 nm.] After 2 h of the polymerization of kinetics, all three monomers had slowed down, which is probably related to gradual oxidation of the photocatalyst.[37,46] However, it has been shown before that it is possible to grow thicker brushes by refreshing the polymerization solution or conducting the polymerization in the presence of an oxygen-

https://dx.doi.org/10.1021/acs.langmuir.9b03536
Langmuir 2020, 36, 4439−4446

consuming agent.[34,37] This indicates that the living nature of the polymers is not lost during PET-RAFT polymerization. Moreover, it has been reported that the rate of polymerization in an oxygen-containing environment in PET-RAFT polymerization conditions is slower and less controlled than that in an inert atmosphere,[47] although such factors clearly do not prevent the smooth growth of thick, homogeneous polymer brushes.

The relatively fast rate and oxygen-tolerant nature of the polymerization allow the SI-PET-RAFT technique to be easily scaled up and used in a wide range of biotechnological and biomedical applications. Moreover, we demonstrate that the SI-PET-RAFT technique can be used with relatively low concentrations of monomer (typically 0.3−1.3 M) and photocatalyst (~39 mM) that creates favorable conditions for its mass application.

Patterning. Another significant advantage of our SI-PET-RAFT approach is that it enables the formation of complex 3D structured polymer brush layers by using a mask and tuning its thickness. This was demonstrated by the growth of poly(HPMA) from a RAFT agent-functionalized surface with a patterning mask. This resulted in a surface with a patterned polymer (Figure S5), with a brush thickness of 30 nm in the exposed regions. In addition, we conducted a control experiment in which a plasma-cleaned silicon substrate without an immobilized RAFT agent was submerged into the polymerization solution and exposed to the same polymerization conditions for 4 h. The sample showed a negligible amount of the absorbed monomer by XPS and an average thickness of 2.1 ± 0.3 nm. This confirms that the polymerization indeed proceeds via the RAFT agent linked to the surface.

Antifouling Properties of Polymer Brushes Synthesized by SI-PET-RAFT. To demonstrate the antifouling properties of the obtained polymer brushes, they were challenged with fluorescently labeled single-protein solutions of streptavidin-Alexa488 conjugate (Str-Alexa488, 0.5 mg·mL^{-1}) and BS albumin-Alexa488 conjugate (BSA-Alexa488, 0.5 mg·mL^{-1}) and with 10-fold diluted biotinylated BS in each case for 15 min. The fouling by biotinylated BS was detected by subsequent exposure to the Str-Alexa488 solution, which binds to the biotin residues of any fouling serum protein present on the surface. The bare silicon surface showed high fluorescence intensities from all three solutions (Figure 4), indicating significant fouling. The fluorescence intensity of all polymer brush-coated samples was low after exposure and similar to the background level measured for unexposed surfaces (Figure 4). The limit of detection of this fluorescent label-based method was determined to be ~0.3 ng·mm^{-2} (corresponding to a fluorescence intensity of about 6 a.u.) by measuring the fluorescence intensity and size of spots of dried drops with known concentrations of fluorescence-labeled proteins (Figure S6). The fluorescence intensities of all polymer brush-coated surfaces after exposure are below the detection limit. Overall, the synthesized polymer brushes showed good antifouling properties (<0.3 ng·mm^{-2}) toward single-protein solutions as well as complex biological liquids such as diluted BS.

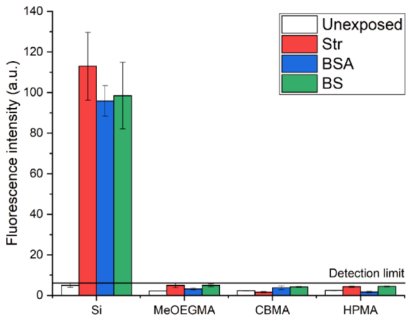

Figure 4. Fluorescence intensity at 500−550 nm of bare silicon, poly(MeOEGMA), thickness: 27 nm, poly(CBMA), thickness: 29 nm, and poly(HPMA), thickness: 26 nm, before and after exposure to solutions of Str-Alexa488 (0.5 mg·mL^{-1}), BSA-Alexa488 (0.5 mg·mL^{-1}), and Str-Alexa488-labeled 10% diluted biotinylated BS.

CONCLUSIONS

We developed a simple light-induced and oxygen-tolerant way for creating antifouling polymer brushes. The brush growth involved a SI-PET-RAFT polymerization. The polymerization was conducted using visible light in an aqueous environment in the presence of EY and TEOA as catalysts. We demonstrated that this approach creates well-defined antifouling polymer brushes based on oligo(ethylene glycol) methacrylate, HPMA. and CBMA. The designed polymer brush coatings showed good antifouling properties in single-protein solutions of BS albumin and streptavidin and also in diluted BS medium. The absence of heavy metal catalysts, the tolerance toward the presence of oxygen, and the phototriggered nature of this polymerization method allow this technique to be used for the construction of patterned surfaces and also to be readily scaled up. We envision that the simplicity of this technique will facilitate the introduction of antifouling coatings based on polymer brushes in mass manufacturing of biomedical and biotechnological devices.

ASSOCIATED CONTENT

Supporting Information

The Supporting Information is available free of charge at https://pubs.acs.org/doi/10.1021/acs.langmuir.9b03536.

SI-PET-RAFT polymerization setup and photopolymerization reactor; simulated C 1s XPS spectrum of APTES, the RAFT agent, and MeOEGMA; images of a patterned layer of poly(HPMA); and fluorescence intensity versus concentration of BSA-Alexa488 spots (PDF)

AUTHOR INFORMATION

Corresponding Authors

Han Zuilhof − *Laboratory of Organic Chemistry, Wageningen University, 6708 WE Wageningen, The Netherlands; School of Pharmaceutical Sciences and Technology, Tianjin University, Tianjin 300072, People's Republic of China; Department of Chemical and Materials Engineering, King Abdulaziz University, 21589 Jeddah, Saudi Arabia;* orcid.org/0000-0001-5773-8506; Email: han.zuilhof@wur.nl

Jacob Baggerman − *Laboratory of Organic Chemistry, Wageningen University, 6708 WE Wageningen, The Netherlands; Aquamarijn Micro Filtration BV, 7201 HB Zutphen, The Netherlands;* orcid.org/0000-0001-9058-6591; Email: jacob.baggerman@wur.nl

https://dx.doi.org/10.1021/acs.langmuir.9b03536
Langmuir 2020, 36, 4439−4446

Authors

Andriy R. Kuzmyn − *Laboratory of Organic Chemistry, Wageningen University, 6708 WE Wageningen, The Netherlands; Aquamarijn Micro Filtration BV, 7201 HB Zutphen, The Netherlands;* orcid.org/0000-0002-1571-2911

Ai T. Nguyen − *Aquamarijn Micro Filtration BV, 7201 HB Zutphen, The Netherlands;* orcid.org/0000-0001-5432-4850

Lucas W. Teunissen − *Laboratory of Organic Chemistry, Wageningen University, 6708 WE Wageningen, The Netherlands;* orcid.org/0000-0003-0018-1211

Complete contact information is available at: https://pubs.acs.org/10.1021/acs.langmuir.9b03536

Author Contributions

The manuscript was written through contributions of all authors. All authors have given approval to the final version of the manuscript.

Funding

The first part of this work has received funding from the European Union's Horizon 2020 research and innovation program under the Marie Sklodowska-Curie grant agreement no. 720325, FoodSmartphone. The second part of this work is part of the Science PPP Fund research program with project number 741.018.105, which is partly financed by the Dutch Research Council (NWO)

Notes

The authors declare no competing financial interest.

■ ACKNOWLEDGMENTS

The authors thank Sidharam Pujari, Jan Willem Borst, Barend van Lagen, and Cees van Rijn for insightful discussions and technical assistance. Esther van Andel is acknowledged for providing biotinylated BS.

■ REFERENCES

(1) Baggerman, J.; Smulders, M. M. J.; Zuilhof, H. Romantic Surfaces: A Systematic Overview of Stable, Biospecific, and Antifouling Zwitterionic Surfaces. *Langmuir* **2019**, *35*, 1072−1084.

(2) Pereira, A. d. l. S.; Rodriguez-Emmenegger, C.; Surman, F.; Riedel, T.; Alles, A. B.; Brynda, E. Use of Pooled Blood Plasmas in the Assessment of Fouling Resistance. *RSC Adv.* **2014**, *4*, 2318−2321.

(3) Rana, D.; Matsuura, T. Surface Modifications for Antifouling Membranes. *Chem. Rev.* **2010**, *110*, 2448−2471.

(4) Homola, J. Surface Plasmon Resonance Sensors for Detection of Chemical and Biological Species. *Chem. Rev.* **2008**, *108*, 462−493.

(5) Yang, J.; Kopeček, J. Design of Smart HPMA Copolymer-Based Nanomedicines. *J. Controlled Release* **2016**, *240*, 9−23.

(6) Xiao, A.; Dhand, C.; Leung, C. M.; Beuerman, R. W.; Ramakrishna, S.; Lakshminarayanan, R. Strategies to Design Antimicrobial Contact Lenses and Contact Lens Cases. *J. Mater. Chem. B* **2018**, *6*, 2171−2186.

(7) Thissen, H.; Gengenbach, T.; du Toit, R.; Sweeney, D. F.; Kingshott, P.; Griesser, H. J.; Meagher, L. Clinical Observations of Biofouling on PEO Coated Silicone Hydrogel Contact Lenses. *Biomaterials* **2010**, *31*, 5510−5519.

(8) Rodriguez-Emmenegger, C.; Avramenko, O. A.; Brynda, E.; Skvor, J.; Alles, A. B. Poly(HEMA) Brushes Emerging as a New Platform for Direct Detection of Food Pathogen in Milk Samples. *Biosens. Bioelectron.* **2011**, *26*, 4545−4551.

(9) Rodriguez Emmenegger, C.; Brynda, E.; Riedel, T.; Sedlakova, Z.; Houska, M.; Alles, A. B. Interaction of Blood Plasma with Antifouling Surfaces. *Langmuir* **2009**, *25*, 6328−6333.

(10) Nguyen, A. T.; Baggerman, J.; Paulusse, J. M. J.; van Rijn, C. J. M.; Zuilhof, H. Stable Protein-Repellent Zwitterionic Polymer Brushes Grafted from Silicon Nitride. *Langmuir* **2011**, *27*, 2587−2594.

(11) Vaisocherová-Lísalová, H.; Surman, F.; Víšová, I.; Vala, M.; Špringer, T.; Ermini, M. L.; Šípová, H.; Šedivák, P.; Houska, M.; Riedel, T.; Pop-Georgievski, O.; Brynda, E.; Homola, J. Copolymer Brush-Based Ultralow-Fouling Biorecognition Surface Platform for Food Safety. *Anal. Chem.* **2016**, *88*, 10533−10539.

(12) Vaisocherová, H.; Ševců, V.; Adam, P.; Špačková, B.; Hegnerová, K.; de los Santos Pereira, A.; Rodriguez-Emmenegger, C.; Riedel, T.; Houska, M.; Brynda, E.; Homola, J. Functionalized Ultra-low Fouling Carboxy- and Hydroxy-functional Surface Platforms: Functionalization Capacity, Biorecognition Capability and Resistance to Fouling from Undiluted Biological Media. *Biosens. Bioelectron.* **2014**, *51*, 150−157.

(13) Chapman, R. G.; Ostuni, E.; Takayama, S.; Holmlin, R. E.; Yan, L.; Whitesides, G. M. Surveying for Surfaces that Resist the Adsorption of Proteins. *J. Am. Chem. Soc.* **2000**, *122*, 8303−8304.

(14) Andree, K. C.; Barradas, A. M. C.; Nguyen, A. T.; Mentink, A.; Stojanovic, I.; Baggerman, J.; van Dalum, J.; van Rijn, C. J. M.; Terstappen, L. W. M. M. Capture of Tumor Cells on Anti-EpCAM-Functionalized Poly(acrylic acid)-Coated Surfaces. *ACS Appl. Mater. Interfaces* **2016**, *8*, 14349−14356.

(15) Jeon, S. I.; Andrade, J. D. Protein—surface Interactions in the Presence of Polyethylene Oxide: II. Effect of Protein Size. *J. Colloid Interface Sci.* **1991**, *142*, 159−166.

(16) Gahtory, D.; Sen, R.; Kuzmyn, A. R.; Escorihuela, J.; Zuilhof, H. Strain-Promoted Cycloaddition of Cyclopropenes with o-Quinones: A Rapid Click Reaction. *Angew. Chem.* **2018**, *130*, 10275−10279.

(17) de los Santos Pereira, A.; Riedel, T.; Brynda, E.; Rodriguez-Emmenegger, C. Hierarchical Antifouling Brushes for Biosensing Applications. *Sens. Actuators, B* **2014**, *202*, 1313−1321.

(18) Kuzmyn, A. R.; de los Santos Pereira, A.; Pop-Georgievski, O.; Bruns, M.; Brynda, E.; Rodriguez-Emmenegger, C. Exploiting End Group Functionalization for the Design of Antifouling Bioactive Brushes. *Polym. Chem.* **2014**, *5*, 4124−4131.

(19) Lísalová, H.; Brynda, E.; Houska, M.; Víšová, I.; Mrkvová, K.; Song, X. C.; Gedeonová, E.; Surman, F.; Riedel, T.; Pop-Georgievski, O.; Homola, J. Ultralow-Fouling Behavior of Biorecognition Coatings Based on Carboxy-Functional Brushes of Zwitterionic Homo- and Copolymers in Blood Plasma: Functionalization Matters. *Anal. Chem.* **2017**, *89*, 3524−3531.

(20) Rodriguez-Emmenegger, C.; Brynda, E.; Riedel, T.; Houska, M.; Šubr, V.; Alles, A. B.; Hasan, E.; Gautrot, J. E.; Huck, W. T. S. Polymer Brushes Showing Non-Fouling in Blood Plasma Challenge the Currently Accepted Design of Protein Resistant Surfaces. *Macromol. Rapid Commun.* **2011**, *32*, 952−957.

(21) van Andel, E.; Lange, S. C.; Pujari, S. P.; Tijhaar, E. J.; Smulders, M. M. J.; Savelkoul, H. F. J.; Zuilhof, H. Systematic Comparison of Zwitterionic and Non-Zwitterionic Antifouling Polymer Brushes on a Bead-Based Platform. *Langmuir* **2019**, *35*, 1181−1191.

(22) Vorobii, M.; de los Santos Pereira, A.; Pop-Georgievski, O.; Kostina, N. Y.; Rodriguez-Emmenegger, C.; Percec, V. Synthesis of Non-fouling poly[N-(2-hydroxypropyl)methacrylamide] Brushes by Photoinduced SET-LRP. *Polym. Chem.* **2015**, *6*, 4210−4220.

(23) Zoppe, J. O.; Ataman, N. C.; Mocny, P.; Wang, J.; Moraes, J.; Klok, H.-A. Surface-Initiated Controlled Radical Polymerization: State-of-the-Art, Opportunities, and Challenges in Surface and Interface Engineering with Polymer Brushes. *Chem. Rev.* **2017**, *117*, 1105−1318.

(24) Kuzmyn, A. R.; Nguyen, A. T.; Zuilhof, H.; Baggerman, J. Bioactive Antifouling Surfaces by Visible-Light-Triggered Polymerization. *Adv. Mater. Interfaces* **2019**, *6*, 1900351.

(25) Laschewsky, A.; Rosenhahn, A. Molecular Design of Zwitterionic Polymer Interfaces: Searching for the Difference. *Langmuir* **2019**, *35*, 1056−1071.

(26) Nguyen, A. T.; Baggerman, J.; Paulusse, J. M. J.; Zuilhof, H.; van Rijn, C. J. M. Bioconjugation of Protein-Repellent Zwitterionic Polymer Brushes Grafted from Silicon Nitride. *Langmuir* **2012**, *28*, 604−610.
(27) Jiang, S.; Cao, Z. Ultralow-Fouling, Functionalizable, and Hydrolyzable Zwitterionic Materials and Their Derivatives for Biological Applications. *Adv. Mater.* **2010**, *22*, 920−932.
(28) Matyjaszewski, K. Advanced Materials by Atom Transfer Radical Polymerization. *Adv. Mater.* **2018**, *30*, 1706441.
(29) Pop-Georgievski, O.; Rodriguez-Emmenegger, C.; Pereira, A. d. l. S.; Proks, V.; Brynda, E.; Rypáček, F. Biomimetic Non-fouling Surfaces: Extending the Concepts. *J. Mater. Chem. B* **2013**, *1*, 2859−2867.
(30) Zamfir, M.; Rodriguez-Emmenegger, C.; Bauer, S.; Barner, L.; Rosenhahn, A.; Barner-Kowollik, C. Controlled Growth of Protein Resistant PHEMA Brushes via S-RAFT Polymerization. *J. Mater. Chem. B* **2013**, *1*, 6027−6034.
(31) Rahane, S. B.; Kilbey, S. M.; Metters, A. T. Kinetics of Surface-Initiated Photoiniferter-Mediated Photopolymerization. *Macromolecules* **2005**, *38*, 8202−8210.
(32) Matsuda, T.; Ohya, S. Photoiniferter-Based Thermoresponsive Graft Architecture with Albumin Covalently Fixed at Growing Graft Chain End. *Langmuir* **2005**, *21*, 9660−9665.
(33) Krause, J. E.; Brault, N. D.; Li, Y.; Xue, H.; Zhou, Y.; Jiang, S. Photoiniferter-Mediated Polymerization of Zwitterionic Carboxybetaine Monomers for Low-Fouling and Functionalizable Surface Coatings. *Macromolecules* **2011**, *44*, 9213−9220.
(34) Niu, J.; Page, Z. A.; Dolinski, N. D.; Anastasaki, A.; Hsueh, A. T.; Soh, H. T.; Hawker, C. J. Rapid Visible Light-Mediated Controlled Aqueous Polymerization with In Situ Monitoring. *ACS Macro Lett.* **2017**, *6*, 1109−1113.
(35) Lueckerath, T.; Strauch, T.; Koynov, K.; Barner-Kowollik, C.; Ng, D. Y. W.; Weil, T. DNA−Polymer Conjugates by Photoinduced RAFT Polymerization. *Biomacromolecules* **2019**, *20*, 212−221.
(36) Niu, J.; Lunn, D. J.; Pusuluri, A.; Yoo, J. I.; O'Malley, M. A.; Mitragotri, S.; Soh, H. T.; Hawker, C. J. Engineering Live Cell Surfaces with Functional Polymers via Cytocompatible Controlled Radical Polymerization. *Nat. Chem.* **2017**, *9*, 537.
(37) Li, M.; Fromel, M.; Ranaweera, D.; Rocha, S.; Boyer, C.; Pester, C. W. SI-PET-RAFT: Surface-Initiated Photoinduced Electron Transfer-Reversible Addition−Fragmentation Chain Transfer Polymerization. *ACS Macro Lett.* **2019**, *8*, 374−380.
(38) Xu, J.; Shanmugam, S.; Duong, H. T.; Boyer, C. Organophotocatalysts for Photoinduced Electron Transfer-Reversible Addition−Fragmentation Chain Transfer (PET-RAFT) Polymerization. *Polym. Chem.* **2015**, *6*, 5615−5624.
(39) Nečas, D.; Klapetek, P. Gwyddion: an Open-source Software for SPM Data Analysis. *Open Physics* **2012**, *10*, 181−188.
(40) Frisch, M. J.; Trucks, G. W.; Schlegel, H. B.; Scuseria, G. E.; Robb, M. A.; Cheeseman, J. R.; Scalmani, G.; Barone, V.; Petersson, G. A.; Nakatsuji, H.; Li, X.; Caricato, M.; Marenich, A. V.; Bloino, J.; Janesko, B. G.; Gomperts, R.; Mennucci, B.; Hratchian, H. P.; Ortiz, J. V.; Izmaylov, A. F.; Sonnenberg, J. L.; Williams, F.; Ding, F.; Lipparini, F.; Egidi, F.; Goings, J.; Peng, B.; Petrone, A.; Henderson, T.; Ranasinghe, D.; Zakrzewski, V. G.; Gao, J.; Rega, N.; Zheng, G.; Liang, W.; Hada, M.; Ehara, M.; Toyota, K.; Fukuda, R.; Hasegawa, J.; Ishida, M.; Nakajima, T.; Honda, Y.; Kitao, O.; Nakai, H.; Vreven, T.; Throssell, K.; Montgomery, J. A., Jr; Peralta, J. E.; Ogliaro, F.; Bearpark, M. J.; Heyd, J. J.; Brothers, E. N.; Kudin, K. N.; Staroverov, V. N.; Keith, T. A.; Kobayashi, R.; Normand, J.; Raghavachari, K.; Rendell, A. P.; Burant, J. C.; Iyengar, S. S.; Tomasi, J.; Cossi, M.; Millam, J. M.; Klene, M.; Adamo, C.; Cammi, R.; Ochterski, J. W.; Martin, R. L.; Morokuma, K.; Farkas, O.; Foresman, J. B.; Fox, D. J. *Gaussian 16*, Revision B.01; Gaussian Inc.: Wallingford, CT, 2016.
(41) Glendening, E. D.; Reed, A. E.; Carpenter, J. E.; Weinhold, F. *NBO*, version 3.1; Gaussian Inc., 2003.
(42) Giesbers, M.; Marcelis, A. T. M.; Zuilhof, H. Simulation of XPS C1s Spectra of Organic Monolayers by Quantum Chemical Methods. *Langmuir* **2013**, *29*, 4782−4788.
(43) Zhao, J.; Gao, F.; Pujari, S. P.; Zuilhof, H.; Teplyakov, A. V. Universal Calibration of Computationally Predicted N 1s Binding Energies for Interpretation of XPS Experimental Measurements. *Langmuir* **2017**, *33*, 10792−10799.
(44) Scheres, L.; Giesbers, M.; Zuilhof, H. Organic Monolayers onto Oxide-Free Silicon with Improved Surface Coverage: Alkynes versus Alkenes. *Langmuir* **2010**, *26*, 4790−4795.
(45) Zhang, Y.; Ye, C.; Li, S.; Ding, A.; Gu, G.; Guo, H. Eosin Y-Catalyzed Photooxidation of Triarylphosphines Under Visible Light Irradiation and Aerobic Conditions. *RSC Adv.* **2017**, *7*, 13240−13243.
(46) Alvarez-Martin, A.; Trashin, S.; Cuykx, M.; Covaci, A.; De Wael, K.; Janssens, K. Photodegradation Mechanisms and Kinetics of Eosin-Y in Oxic and Anoxic Conditions. *Dyes Pigm.* **2017**, *145*, 376−384.
(47) Zhou, J.; Ye, L.; Lin, Y.; Wang, L.; Zhou, L.; Hu, H.; Zhang, Q.; Yang, H.; Luo, Z. Surface Modification PVA Hydrogel with Zwitterionic via PET-RAFT to Improve the Antifouling Property. *J. Appl. Polym. Sci.* **2019**, *136*, 47653.

https://dx.doi.org/10.1021/acs.langmuir.9b03536
Langmuir 2020, 36, 4439−4446